www.czasopisma.pan.pl PAN POLSKA AKADEMIA NAUK www.journals.pan.pl

Archives of Acoustics Online First April 24, 2024 doi: 10.24425/aoa.2024.148794

Research Paper

Evaluation Modeling of Electric Bus Interior Sound Quality Based on Two Improved XGBoost Algorithms Using GS and PSO

Enlai ZHANG[(1),(2)], Yi CHEN[(1)], Liang SU[(3)*], Ruoyu ZHONGLIAN[(1)], Xianyi CHEN[(1)], Shangfeng JIANG[(1)**]

[(1)] *School of Mechanical and Automotive Engineering, Xiamen University of Technology*
Xiamen, China

[(2)] *Xiamen Key Laboratory of Robot Systems and Digital Manufacturing*
Xiamen, China

[(3)] *Bus Engineering Research Institute, Xiamen King Long United Automotive Industry Co., Ltd*
Xiamen, China

Corresponding Authors' e-mails: *slkinglong@163.com, **jiangsfa@163.com

(*received October 10, 2023; accepted March 15, 2024; published online April 24, 2024*)

There is no doubt that traffic noise has become one of the main sources of urban noise, and the electric bus, as an important means of transport frequently used by people in daily life, has a direct impact on the psychological and auditory health of passengers due to its interior noise characteristics. Consequently, studying electric bus sound quality is an important way to improve vehicle performance and comfort. In this paper, eight electric buses were selected and 64 noise samples were measured. Acoustic comfort was taken as an evaluation index, professionals were organized to complete the subjective evaluation tests for all noise samples based on rank score comparison (RSC). And nine psycho-acoustic objective parameters such as loudness, sharpness and roughness were calculated using ArtemiS software to establish the sound quality database of electric buses. Aiming at the practical application requirements of high-precision modeling of acoustic comfort in vehicles, this paper presented two improved extreme gradient boosting (XGBoost) algorithms based on grid search (GS) method and particle swarm optimization (PSO), respectively, with objective parameters and acoustic comfort as input and output variables, and established three regression models of standard XGBoost, GS-XGBoost and PSO-XGBoost through data training. Finally, the calculation results of three indexes of average relative error, square root error and correlation coefficient indicate that the proposed PSO-XGBoost model is significantly better than GS-XGBoost and standard XGBoost, with its prediction accuracy as high as 97.6 %. This model is determined as the evaluation model of interior acoustic comfort for this case, providing a key technical support for future sound quality optimization of electric buses.

Keywords: electric bus; sound quality; acoustic comfort; GS-XGBoost; PSO-XGBoost.

1. Introduction

As an important form of green transport, electric bus has been developing rapidly domestically in recent decades. However, there is serious homogenization in the same class of models in terms of motor electric control, battery range, vehicle safety, and other conventional performance measures, resulting in increased industry competition. Focusing on internal quality improvement and improving user experience have become a differentiation strategy for electric bus development, shifting focus from high speed to high quality. Practice demonstrates that vehicle interior noise quality is the most direct factor affecting people's subjective experiences. An excellent acoustic environment is conducive to the physical and mental health of drivers and passengers, and significantly improves users' satisfaction with the vehicle (Steinbach, Altinsoy, 2019;

Zhang *et al.*, 2021). Therefore, the change of electric bus noise control from noise reduction to sound quality is of great application importance in establishing the core competitiveness of vehicle products.

Because driving motor replaces conventional engine, the noise inside electric bus is more pronounced due to the absence of engine masking effect, and many noise types that are not easily to be detected in the fuel bus appear more prominent in electric buses, such as air conditioning noise, electromagnetic noise, tire noise and mechanical transmission noise (Shi *et al.*, 2018; Zhang *et al.*, 2022b). In particular, the motor electromagnetic noise is characterized by high current, variable frequency regulation and high magnetic density. Its spectral characteristics often fall within the sensitive range of human ears to noise, leading to a harsh subjective feeling, which has a significant negative impact on the whole vehicle acoustic comfort (Doleschal, Verhey, 2022). It can be concluded that it is urgent and imperative for the development of electric buses to improve interior sound quality.

It is well-known that subjective and objective evaluations are the main issues in sound quality research. Subjective evaluation can directly reflect people's auditory feelings, but the evaluation process requires a lot of human and material resources, and its results are susceptible to the psychological and physiological factors of evaluators (Zhang *et al.*, 2018). Therefore, on the basis of obtaining noise database, using objective parameters as independent variables and subjective evaluation test results as dependent variables, establishing a functional relationship between them through data fitting, namely, a quantifiable mapping model for acoustic quality evaluation, is a hot direction in current vehicle sound quality research.

Sound quality modeling approaches can be broadly classified into two categories: the first is based on mathematical statistics, mainly including multiple linear regression (Zhang *et al.*, 2018), Kriging model (Zhang *et al.*, 2020) and grey system theory (Chen *et al.*, 2012); the second category is based on machine learning algorithms to simulate the ability of human neural networks to extract and process information features. Since the structure of the human ear resembles a nonlinear and complex sound receiver, studies have indicated that the nonlinear mapping relationship between subjective and objective evaluations can more accurately describe real auditory perception (Wang, 2009; Pourseiedrezaei *et al.*, 2021), in which the algorithms involved in this category include back-propagation neural networks (BPNN) (Pourseiedrezaei *et al.*, 2021; Zhang *et al.*, 2016), support vector machine (Liang *et al.*, 2020; Ding *et al.*, 2023), deep learning (Huang *et al.*, 2016; 2021), and extreme gradient boosting (XGBoost) (Wang *et al.*, 2022), etc. For example, Huang *et al.* (2020) and Kim and Lee (2022), respectively, used convolutional neural network to establish quantitative evaluation models of in-vehicle annoyance and driving sound quality. In the past two years, XGBoost has been applied to nonlinear modeling of vehicle annoyance due to its excellent fitting performance and generalization ability (Wang *et al.*, 2022; Zhang *et al.*, 2023b). Wang *et al.* (2022) collected interior noise at different speeds to build a nonlinear XGBoost-based annoyance model using subjective and objective database.

XGBoost, first proposed by prof. Chen in 2016, uses second-order Taylor expansion to optimize the objective function and introduces regularization terms to improve the model's generalization ability and to effectively control its over-fitting problem (Chen, Guestrin, 2016). In our past researches, for 64 electric bus sound quality modeling applications, BPNN and standard XGBoost were utilized to establish two high-precision interior acoustic comfort prediction models with average relative error of 4.35 % and 4.67 %, respectively, (Zhang *et al.*, 2022a; 2023a). To make the prediction model more accurate and robust, based on the existing standard XGBoost regression model, we explore the combination of XGBoost with grid search (GS) and particle swarm optimization (PSO) to optimize the mapping model parameters. Thus, propose two improved algorithms of GS-XGBoost and PSO-XGBoost, to further expand the applicability of XGBoost in the field of vehicle sound quality.

2. Subjective and objective evaluations

2.1. Noise sample collection

Eight different types of electric buses, denoted A to H, were selected for noise testing. As there is no bus sound quality standardized test, the test and evaluation methods for city bus internal noise (XMQT075-2021) were used for reference. During the test, we chose two different working conditions with the air conditioner on and off. Measurements were taken at two positions: the driver's seat and the rear seat, as illustrated in Fig. 1. The sample buses operated at constant speeds of 30 km/h and 50 km/h on a professional track. When the tested bus was running stably, its interior noise signals were acquired by Squadriga II binaural acquisition system with a headset BHS II, as shown in Fig. 2.

2.2. Evaluation process

Obviously, in this test, the signal samples collected are transmitted to the human ear after the comprehensive superposition of various noise sources such as tire-road noise and electromagnetic noise. Since the

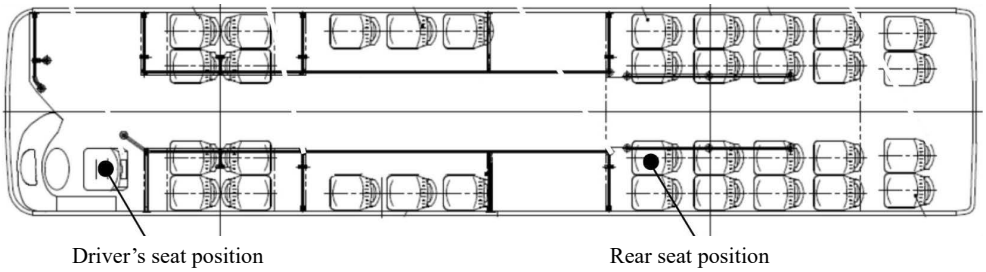

Fig. 1. Distribution of the two measuring points.

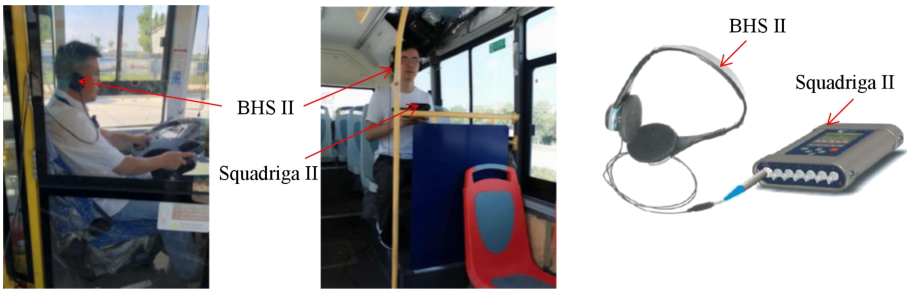

Fig. 2. Test scenes and measuring instruments.

human ear may feel auditory fatigue due to exposure to longer noise samples, pre-processing steps such as interception and screening were completed before the evaluation test, and a total of 64 in-vehicle noise samples from electric buses, each with a duration of 5 seconds, were finally acquired (Zhang *et al.*, 2022a; 2023a). To avoid the potential information influence of measuring points, speeds and working conditions of noise samples on sound quality evaluation tests, all samples were re-coded and randomly ordered. The results are shown in Table 1.

Table 1. Random order of all noise samples.

AFD3	AFD5	AFM3	AFM5	AND3	AND5	ANM3	ANM5
49	18	9	37	1	32	13	21
BFD3	BFD5	BFM3	BFM5	BND3	BND5	BNM3	BNM5
44	27	36	20	46	8	30	41
CFD3	CFD5	CFM3	CFM5	CND3	CND5	CNM3	CNM5
24	19	10	26	54	48	51	2
DFD3	DFD5	DFM3	DFM5	DND3	DND5	DNM3	DNM5
31	55	40	4	62	12	29	57
EFD3	EFD5	EFM3	EFM5	END3	END5	ENM3	ENM5
3	34	15	22	58	11	35	63
FFD3	FFD5	FFM3	FFM5	FND3	FND5	FNM3	FNM5
60	43	7	52	5	16	64	25
GFD3	GFD5	GFM3	GFM5	GND3	GND5	GNM3	GNM5
23	33	28	61	17	59	39	53
HFD3	HFD5	HFM3	HFM5	HND3	HND5	HNM3	HNM5
14	47	6	45	38	50	42	56

Note – the code meaning is as follows: AND3 (number 1) represents the noise sample acquired from an electric bus in the driver's position at 30 km/h with the air conditioner turned on.

The sound quality evaluation process consists of subjective evaluation and objective acoustic parameter calculation. In this case, the rank score comparison (RSC) was used for subjective evaluation tests of electric bus noise samples. Acoustic comfort was taken as the evaluation index, divided into five comfort levels: poor, accepted, satisfied, good, and excellent, and each further added two values for each level. Thus, the acoustic comfort level range within [1, 10] was constituted. The jury for this subjective evaluation test was composed of NVH engineers, drivers and acoustic experts with rich experience in bus noise. It is well-known that different people may yield different evaluation results for the same noise sample due to psychological and emotional influences and cognitive differences. In order to ensure the validity and reliability of the subjective evaluation results, four measures were taken: (1) increase the number of acoustic experts, including university professors and senior engineers, who accounted for nearly half of the jury; (2) to avoid mutual interference between evaluators, only one evaluator was allowed to participate in the subjective evaluation in a specialized testing room; (3) for reducing the discreteness of subjective activities, the evaluation test was divided into two stages, i.e., pre-evaluation and final evaluation. In the pre-evaluation test, acoustic experts conducted subjective evaluation on the two selected comparison noise samples (numbered 34 and 49 in Table 1) and assigned appropriate acoustic comfort values. In the final evaluation test, all evaluators first played the two comparison samples and paid attention to their acoustic comfort values, and then combined them with their subjective feelings to complete the scoring of 64 noise samples in turn; (4) in the

data statistics stage, Spearman correlation coefficient and K-means clustering were used to analyze the data characteristics of all the evaluators, and after excluding the data with correlation coefficients lower than 0.7 and low similarity, the data of the remaining evaluators were averaged, that is, the acoustic comfort values of all noise samples were finally obtained, as listed in Table 2.

In terms of objective evaluation, ArtemiS software by HEAD was applied to calculate objective psychoacoustic parameters of all noise samples, including linear sound pressure level (dB), A-weighted sound pressure level (dB(A)), loudness (sone), sharpness (acum), roughness (asper), fluctuation strength (vacil), articulation index (AI, %), impulsiveness (iu), and relative approach (cPa), corresponding to independent variables x_1, x_2, x_3, x_4, x_5, x_6, x_7, x_8, and x_9, respectively. The objective evaluation results of all noise samples are displayed in Table 3.

Table 2. Acoustic comfort values of 64 noise samples after subjective evaluations.

1	2	3	4	5	6	7	8
5.17	3.33	6.42	5.33	4.67	3.25	2.58	3.42
9	10	11	12	13	14	15	16
5.75	5.25	4.58	4.83	4.42	4.67	2.33	5.42
17	18	19	20	21	22	23	24
3.17	7.25	2.92	7.08	4.92	2.08	5.33	3.84
25	26	27	28	29	30	31	32
2.33	3.08	3.92	2.5	4.25	5.08	3.92	2.5
33	34	35	36	37	38	39	40
2.42	4.25	1.75	7.5	5.08	1.42	2.58	6.75
41	42	43	44	45	46	47	48
6.92	2.5	4	5.17	2.33	3.84	4.83	3.08
49	50	51	52	53	54	55	56
7.67	4.12	3.67	2.58	2.67	4.25	5.58	1.92
57	58	59	60	61	62	63	64
5.33	3.58	2.58	5.32	4.33	4.84	1.58	3.13

Table 3. Objective parameter calculation results of 64 noise samples.

Sample	x_1	x_2	x_3	x_4	x_5	x_6	x_7	x_8	x_9
1	105.43	73.11	29.6	1.6	0.105	0.087	43.6	0.398	19.1
2	108.24	77.59	43.2	2.3	0.122	0.108	18.8	0.409	19.7
3	96.73	61.18	15.8	1.34	0.071	0.0722	79.4	0.57	15.7
4	108.53	74.4	34.1	1.84	0.0958	0.112	34.8	0.36	20.2
5	102	67.51	24.5	1.62	0.0827	0.0795	54.6	0.376	17.9
6	89.57	66.71	20.9	1.39	0.131	0.061	62.4	0.286	15.7
7	95.65	67.97	24.3	1.6	0.105	0.0623	55.7	0.334	16.3
8	102.38	74.24	34	1.99	0.12	0.0645	31.4	0.394	18.4
9	100.06	69.54	22.2	1.42	0.0951	0.0793	59.9	0.37	16.3
10	102.46	69.85	25.2	1.73	0.0974	0.0755	48.5	0.408	15.9
11	99.03	72.45	28.6	1.84	0.122	0.0638	41.2	0.343	16.6
12	107.04	72.78	33.4	1.78	0.0943	0.0954	37.9	0.431	20.3
13	100.57	70.76	25.7	1.72	0.106	0.0824	47.5	0.387	16.7
14	95.06	63.03	18.2	1.55	0.0878	0.0727	67.4	0.279	15.6
15	91.63	69.81	22.5	1.28	0.117	0.0638	63.1	0.358	13.7
16	106.93	72.01	33.7	1.74	0.0932	0.0967	41.2	0.465	21.4
17	97.07	69.2	25.3	1.8	0.106	0.0576	46	0.351	16.2
18	105.61	72.5	28.4	1.51	0.1	0.0847	47.2	0.414	19.1
...	...	...	...	...	...	...	...	...	...
50	101.53	71.83	31.6	1.59	0.117	0.0744	43.1	0.264	18.6
51	100.35	71.11	26.9	1.81	0.112	0.0664	44.8	0.393	16
52	101.18	73.57	35.3	1.86	0.123	0.0761	36	0.492	20.6
53	101.12	74.08	35.4	1.78	0.12	0.0649	35.2	0.349	18.4
54	107.55	72.01	31.6	2.01	0.097	0.0795	35.4	0.46	19.7
55	107.61	73.21	32	1.67	0.0889	0.092	41.8	0.474	20.8
56	95.57	74.79	31.5	1.67	0.157	0.0793	36.8	0.225	17.6
57	106.14	75.12	35	2.06	0.102	0.111	30.8	0.363	18.7
58	97.78	70.22	26.4	1.86	0.112	0.0574	44.9	0.343	16
59	103.2	78.46	42.8	1.68	0.104	0.106	35.3	0.322	19.2
60	101.53	65.3	21.7	1.41	0.0728	0.0804	66.5	0.464	18.9
61	100.28	72.34	29.3	1.58	0.1	0.0704	46.4	0.306	17.6
62	101.65	70.62	25.5	1.77	0.0837	0.0845	50.5	0.429	18.4
63	97.08	78.18	38.1	1.96	0.165	0.0779	26.5	0.334	16.3
64	96.98	70.89	29.9	1.72	0.117	0.0626	44.4	0.363	16.7

3. XGBoost and its improved algorithms

3.1. XGBoost

XGBoost is implemented based on the gradient boosting decision tree using the integration method of boosting. The modeling idea is to first define an objective function, then find the best tree model to fit the residual error of the previous prediction in each iteration, and pursue to minimize the objective function so that predicted value is as close to targeted value as possible. Its theory and implementation process are detailed in the corresponding reports (Wang *et al.*, 2022; Zhang *et al.*, 2023b).

XGBoost is a powerful and highly flexible machine learning model that is significantly affected by several structural parameters. These structural parameters are categorized into weak learner parameters and boosting framework parameters, mainly including the maximum depth of the decision tree, the maximum number of leaf nodes, the learning rate, etc. Different combinations of these parameters may result in the model exhibiting very different levels of performance on different tasks. Due to the complex interactions between these parameters, manually tuning them to achieve optimal performance becomes extremely complex in the high-dimensional parameter space. Therefore, the introduction of intelligent optimization algorithms to efficiently search for optimal combinations of structural parameters with optimal performance is necessary to improve the prediction accuracy of the model.

3.2. Improved XGBoost based on GS

The grid search (GS) method introduced in this section is an intelligent algorithm for structural parameter optimization (Wang *et al.*, 2020). The steps for combining it with XGBoost mainly include: traversing all possible values of specified parameters to form a parameter grid. Then, all parameter combinations in the grid search are put into the model successively for prediction, and the one with the smallest error among all parameter combinations is taken as the best parameter. Finally, a new GS-XGBoost model is established with the best parameters, thus realizing the parameter optimization of XGBoost (Das *et al.*, 2014). The proposed algorithm of GS-XGBoost is illustrated in Fig. 3.

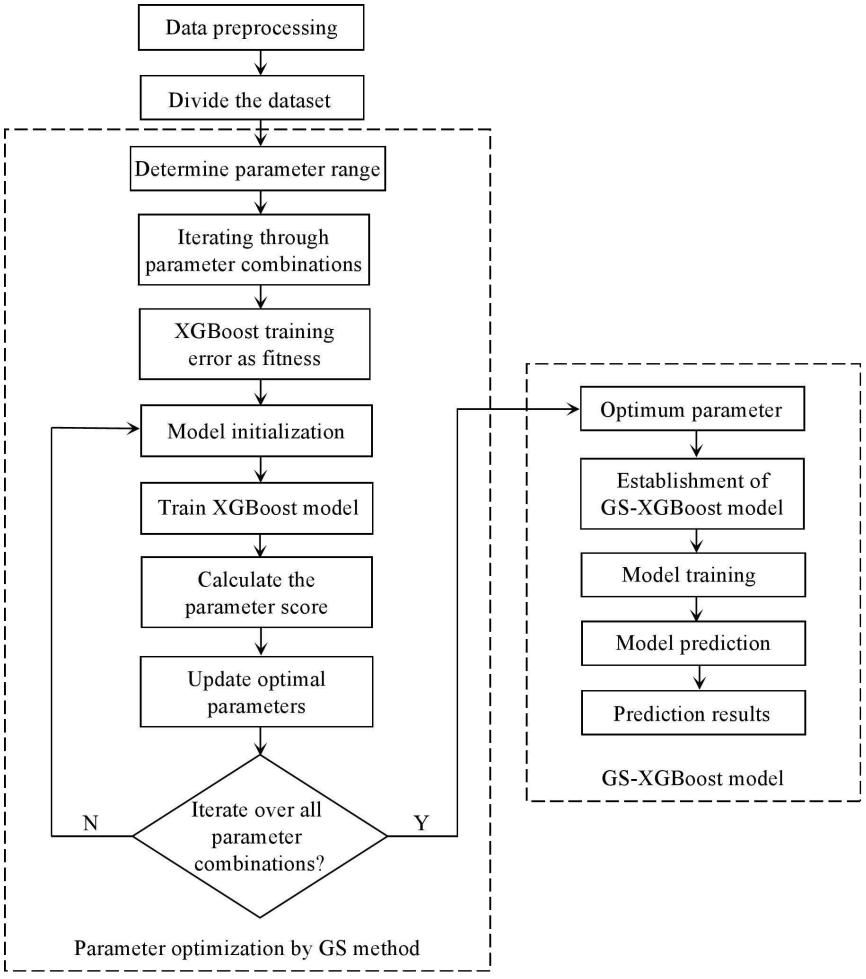

Fig. 3. Flow block diagram of GS-XGBoost algorithm.

Table 4. Structural parameter and range for GS-XGBoost.

Parameter	Value and range	Meaning of structural parameters
Learning_rate	(0.2, 0.3) with step of 0.01	Learning rate
Max_depth	(3, 10) with step of 1	Maximum depth of the tree
Subsample	(0.6, 0.9) with step of 0.01	Percentage of randomly selected samples
Colsample_bytree	(0.6, 0.9) with step of 0.01	Feature random sampling ratio
alpha	(0, 0.01)	L_1 canonical term parameters
lamba	(0, 1)	L_2 canonical term parameters

According to the above description, GS is an exhaustive method that involves exploring all possible combinations of structural parameters and then using these parameter sets for model prediction. Based on the characteristics of GS, the iteration time for optimizing XGBoost increases significantly with the number and range of parameters. Therefore, in this case, after going through the initial manual search, the parameters to be optimized and their respective ranges are identified. The structural parameters involved and their ranges are listed in Table 4.

3.3. Improved XGBoost based on PSO

Particle swarm optimization (PSO) is a population intelligence-based algorithm that optimizes objective function by simulating the collective behavior of birds (Zhang *et al.*, 2016; Madvari *et al.*, 2022). In principle, it is assumed that n particle populations in D-dimensional space are generated, the position of each particle is solved as $X_i = (x_i^1, x_i^2, ..., x_i^D)$, and the velocity value of the i-th particle is $V_i = (v_i^1, v_i^2, ..., v_i^D)$, the extreme values of individual and population are $P_i = (p_i^1, p_i^2, ..., p_i^D)$ and $P_g = (p_g^1, p_g^2, ..., p_g^D)$, respectively. Then, according to the given fitness function, the fitness of each particle is calculated and the optimal values of individual and population are continuously updated. Finally, the remaining particles update their positions and velocities according to the current extreme values. The position and velocity of a particle are updated by the following equations:

$$V_{id}^{k+1} = \omega V_{id}^k + c_1 r_1 (P_{id}^k - X_{id}^k) + c_2 r_2 (P_{gd}^k - X_{id}^k), \quad (1)$$

$$X_{id}^{k+1} = X_{id}^k + V_{id}^{k+1}, \quad (2)$$

where ω is the inertia factor; $i = 1, 2, 3, ..., n$, and n is the number of particles; $d = 1, 2, 3, ..., D$, and D is the dimension of the particle swarm; k is the number of current iterations; V_{id} and X_{id} stand, respectively, for the velocity and position of the particle id; P_{id} and P_{gd} are the optimal position experienced by particle id and the entire particle swarm; c_1 and c_2 represent learning factors; and r_1 and r_2 are random numbers distributed in the interval [0, 1]. The basic parameters of PSO are listed in Table 5.

Compared with the GS method, PSO can improve search efficiency through the collaborative and following behavior of the population, thereby reducing the time and space complexity of parameter search. And thus, for PSO, the influence of the number and range of parameters on optimization time is relatively small, mainly depending on the optimization objectives and constraints set. In this case, in order to construct the PSO-XGBoost regression model with high accuracy and strong generalization capability, the types and ranges of structural parameters are expanded and presented as in Table 6.

The proposed regression modeling process of PSO-XGBoost consists of three steps (see Fig. 4):

Step 1: preprocess the sound quality data and divide it into training and testing sets, followed by determining the model parameters and their search ranges as shown in Table 6.

Step 2: take the training error of XGBoost model as fitness, initialize the parameters of PSO shown in Table 5, and obtain the optimal fitness parameters in the solution space. Finally, the convergence condition is whether the maximum number of iterations or accuracy requirements is reached, and the model's best parameters are output when the condition is satisfied; otherwise the algorithm continues to perform the above optimization search steps.

Step 3: establish a new PSO-XGBoost model based on the optimal parameters, train the model, and output its prediction results.

Table 5. Pre-selected parameters of PSO.

Parameter	Value	Meaning of structural parameters
ω	0.5	Inertia factor
c_1	0.5	Learning factor
c_2	0.5	Learning factor
swarmsize	20	Number of populations
Max Stallterations	50	Maximum number of iterations

Table 6. Structural parameter and range for PSO-XGBoost.

Parameter	Value range	Meaning of structural parameters
n_estimators	(50, 100)	Number of trees
Learning_rate	(0.001, 0.5)	Learning rate
Max_depth	(1, 5)	Maximum depth of the tree
Subsample	(0.1, 1)	Percentage of randomly selected samples
Colsample_bytree	(0, 0.8)	Feature random sampling ratio
alpha	(1, 10)	L_1 canonical term parameters
lamba	(0, 10)	L_2 canonical term parameters
gamma	(0, 15)	Minimum drop value of loss function required for node splitting
Max_delta_step	(0, 10)	Maximum step size for each tree weight change
Min_child_weight	(0, 10)	Sum of sample weights of minimum leaf nodes

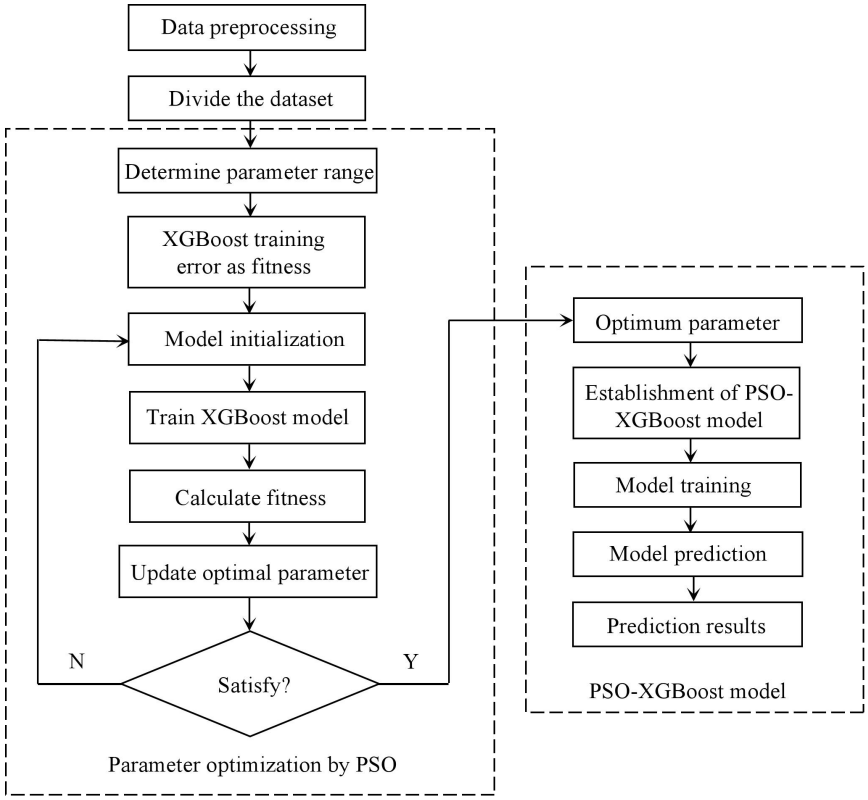

Fig. 4. Flow block diagram of PSO-XGBoost algorithm.

4. Acoustic comfort evaluation modeling and prediction

4.1. Optimum structural parameters

The purpose of this section is to develop a new model for electric bus acoustic comfort with high accuracy based on the above established sound quality database, where objective psycho-acoustic parameters and acoustic comfort are the input and output dependent variables of the model, respectively, corresponding to x_1 to x_9 in Tables 2 and 3. The database is divided into two data sets by noise samples: the first to 56th sample data for training and the 57th to 64th sample data for testing. The algorithms of standard XGBoost, GS-XGBoost, and PSO-XGBoost were performed, respectively, on the MATLAB platform, with their corresponding model parameters and imported data were set. After running the codes, the optimal structural parameters of each regression model were obtained. Finally, the results are listed in Table 7.

4.2. Evaluation indicators of model accuracy

In order to evaluate and compare the algorithm performance of the above three regression models, average relative error (ARE), root mean square error (RMSE) and correlation coefficient (R^2) are taken as the accuracy indexes to measure the models, and their calculation formulas are expressed further, where y_k

Table 7. Optimized structural parameters for two regression models.

Regression model	Structural parameter variable	Optimal structural parameters
GS-XGBoost	Learning_rate	0.285
	Max_depth	3
	Subsample	0.9
	Colsample_bytree	0.8
	alpha	0
	lamba	1
PSO-XGBoost	n_estimators	71
	Learning_rate	0.499
	Max_depth	2
	Subsample	0.739
	Colsample_bytree	0.691
	lamba	7.259
	alpha	1.644
	gamma	0.181
	Max_delta_step	5.689
	Min_child_weight	3.024

and z_k represent the test and predicted values, respectively.

The smaller the values of ARE and RMSE, describing the degree of deviation between predicted and test values, the higher the model prediction accuracy, and they are defined by the equations:

$$e_{\mathrm{ARE}} = \frac{1}{N}\sum_{k=1}^{N}\left|\frac{y_k - z_k}{y_k}\right| \times 100\,\%, \tag{3}$$

$$e_{\mathrm{RMSE}} = \sqrt{\frac{\sum_{k=1}^{N}(z_k - y_k)^2}{N}}. \tag{4}$$

R^2 is a parameter measuring the closeness of two data groups, calculated by Eq. (5), and its higher value indicates the higher model's fitting accuracy:

$$R^2_{X,Y} = \frac{E((X-EX)(Y-EY))}{\sqrt{D(X)}\sqrt{D(Y)}}, \tag{5}$$

where E represents the variable's mathematical expectation; D is the symbol for variance; $E((X-EX)(Y-EY))$ is the covariance between the random variables X and Y.

4.3. Acoustic comfort prediction results and comparison

Based on the testing set, the evaluation indexes of regression models trained by standard XGBoost, GS-XGBoost, and PSO-XGBoost were calculated. The predicted values and accuracy results are obtained and listed in Table 8.

Table 8 visually indicates that the prediction accuracy of standard XGBoost, GS-XGBoost, and PSO-XGBoost models all meet the application requirements of maximum relative error (MRE) and ARE less than 10 % and 5 %, respectively. For the standard XGBoost model, MRE and ARE are 8.53 % and 4.67 %, respectively. For the GS-XGBoost model, MRE is 8.83 %, 0.3 % higher than the standard XGBoost, and ARE is 3.64 %, 1.03 % lower than the standard XGBoost. For the PSO-XGBoost model, MRE and ARE are 6.33 % and 2.30 %, respectively, which are 2.2 % and 2.37 % lower than the standard XGBoost. In addition,

Table 8. Prediction results of three regression models.

Standard XGBoost (Zhang *et al.*, 2023a)				GS-XGBoost		PSO-XGBoost	
Sample	Target value	Predicted value	Relative error [%]	Predicted value	Relative error [%]	Predicted value	Relative error [%]
57	5.33	5.20	2.44	5.24	1.69	5.35	0.38
58	3.58	3.59	0.28	3.53	1.40	3.66	2.23
59	2.58	2.8	8.53	2.54	1.55	2.66	3.10
60	5.32	5.68	6.77	5.79	8.83	5.22	1.88
61	4.33	4.02	7.16	4.04	6.70	4.35	0.46
62	4.84	4.56	5.79	4.79	1.03	4.94	2.06
63	1.58	1.55	1.90	1.67	5.70	1.48	6.33
64	3.13	3.27	4.47	3.06	2.23	3.07	1.92

according to Eq. (4), the RMSEs of PSO-XGBoost and GS-XGBoost models correspond to 0.0843 and 0.2039, which are 0.1365 and 0.0169 smaller than 0.2208 of the standard XGBoost model, respectively. It can be concluded that the prediction accuracy of the three established models can be ranked from high to low as follows: PSO-XGBoost > GS-XGBoost > standard XGBoost.

In terms of model's fitting accuracy, three correlation coefficients of standard XGBoost, GS-XGBoost and PSO-XGBoost are calculated by Eq. (5) as 0.9848, 0.9881, and 0.998. Figures 5–7 show the fitting results of the above three models, in which solid dot is the sample data corresponding to test and predicted values, and orange solid and blue dotted lines represent the best fitting position and the error range of 10 %, respectively. It can be seen that the predicted data point distribution of PSO-XGBoost model is closest to the best fitting line, followed by GS-XGBoost model, and the last is the standard XGBoost model, indicating that the three models perform consistently in terms of fitting accuracy with respect to prediction accuracy.

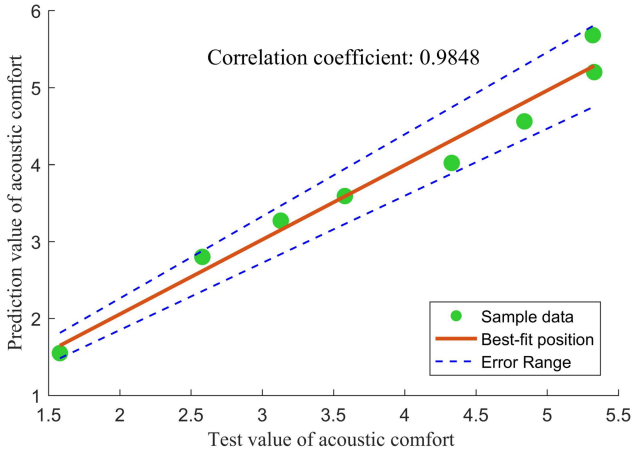

Fig. 5. Fitting result of standard XGBoost model.

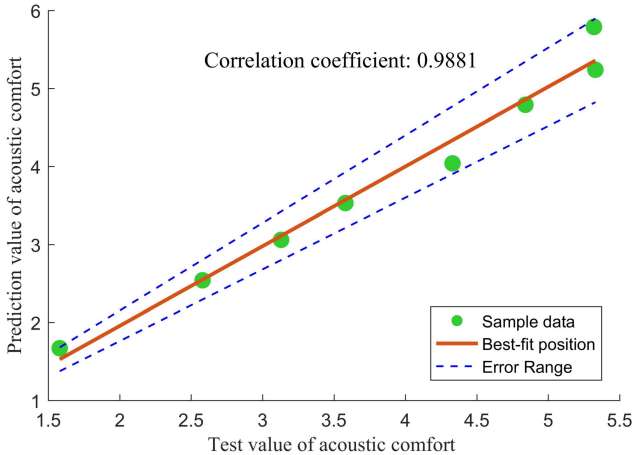

Fig. 6. Fitting result of GS-XGBoost model.

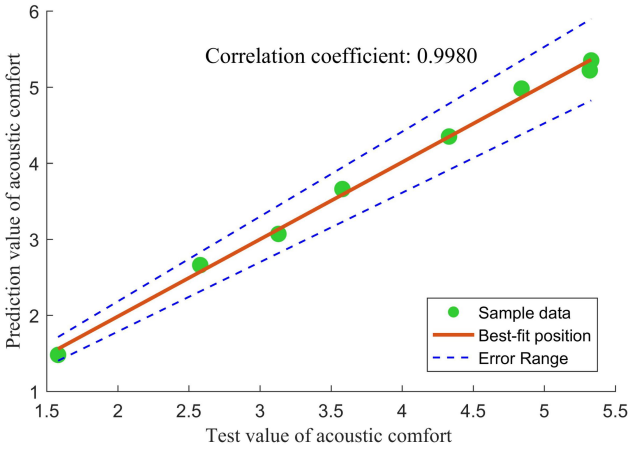

Fig. 7. Fitting result of PSO-XGBoost model.

To sum up, for the acoustic comfort modeling of electric bus, the prediction and fitting accuracy of GS-XGBoost model and PSO-XGBoost model are higher than that of standard XGBoost model, proving the improved XGBoost algorithms have obvious application effectiveness and superiority. Therefore, the established PSO-XGBoost model is finally adopted as the acoustic comfort evaluation model for this case, which provides a new technical support for research on electric bus interior sound quality.

5. Conclusions and future work

The electric bus is widely used and its interior sound quality research is an emerging field. Establishing sound quality prediction model aims to overcome the shortcomings of subjective evaluation tests with tedious processes and susceptible results. Based on the subjective and objective evaluation database, for improving model's accuracy and robustness, two intelligent algorithms, GS and PSO, were introduced to improve the XGBoost algorithm by optimizing model parameters. This led to establishing the acoustic comfort evaluation model for electric bus based on GS-XGBoost and PSO-XGBoost. Finally, ARE, RMSE, and R^2 of the predicted results demonstrates that PSO-XGBoost model has the best prediction and fitting accuracy, followed by GS-XGBoost model, proving the effectiveness and applicability of the improved XGBoost algorithms.

Future research will primarily focus on two aspects: one is to collect noise signals in unsteady conditions, and further evaluate the generalization abilities of the improved XGBoost algorithms in characterizing dynamic sound quality; second will consider more observation points for improving sound quality data scale, and combine the proposed algorithms with semi-supervised learning to explore online modeling methods for electric bus interior sound quality.

Acknowledgments

The authors would like to thank the Bus Engineering Research Institute of Xiamen King Long United Automotive Industry Co., Ltd for providing bus prototypes and signal acquisition instruments, and for organizing engineers to participate in subjective evaluation tests.

Fundings

The work was supported by the National Natural Science Foundation of China (12004136), the Natural Science Foundation of Fujian Province (2023J011438, 2023J011437), the Key Research and Industrialization Project of Technological Innovation in Fujian Province (2023G013), the Major Educational Research Project of Fujian Province (FBJY20230154), and the Science and Technology Project for High-level Talents of XMUT (YKJ22017R).

Conflict of interest

The authors declare that they have no conflict of interest.

References

1. Chen S.M., Wang D.F., Liang J. (2012), Sound quality analysis and prediction of vehicle interior noise based on grey system theory, *Fluctuation and Noise Letters*, **11**(2): 1250016, doi: 10.1142/S0219477512500162.
2. Chen T.Q., Guestrin C. (2016), XGBoost: A scalable tree boosting system, [in:] *KDD '16: Proceedings of the 22nd ACM SIGKDD International Conference on Knowledge Discovery and Data Mining*, pp. 785–794, doi: 10.1145/2939672.2939785.
3. Das G., Pattnaik P.K., Padhy S.K. (2014), Artificial neural network trained by particle swarm optimization for non-linear channel equalization, *Expert Systems with Applications*, **41**(7): 3491–3496, doi: 10.1016/j.eswa.2013.10.053.
4. Ding F., Xie W.T., Xie X.P. (2023), Research on optimization of car door closing sound quality based on the integration of structural simulation and test, [in:] *Proceedings of the Institution of Mechanical Engineers, Part D: Journal of Automobile Engineering*, **237**(6): 1378–1390, doi: 10.1177/09544070221088370.
5. Doleschal F., Verhey J.L. (2022), Pleasantness and magnitude of tonal content of electric vehicle interior sounds containing subharmonics, *Applied Acoustics*, **185**: 108442, doi: 10.1016/j.apacoust.2021.108442.
6. Huang H.B., Huang X.R., Li R.X., Lim T.C., Ding W.P. (2016), Sound quality prediction of vehicle interior noise using deep belief networks, *Applied Acoustics*, **113**: 149–161, doi: 10.1016/j.apacoust.2016.06.021.
7. Huang H.B., Wu J.H., Lim T.C., Yang M.L., Ding W.P. (2021), Pure electric vehicle nonstationary interior sound quality prediction based on deep CNNs with an adaptable learning rate tree, *Mechanical System and Signal Processing*, **148**: 107170, doi: 10.1016/j.ymssp.2020.107170.
8. Huang X.R., Huang H.B., Wu J.H., Yang M.L., Ding W.P. (2020), Sound quality prediction and improving of vehicle interior noise based on deep convolutional neural networks, *Expert Systems with Applications*, **160**: 113657, doi: 10.1016/j.eswa.2020.113657.
9. Kim D., Lee J. (2022), Predictive evaluation of spectrogram-based vehicle sound quality via data augmentation and explainable artificial Intelligence: Image color adjustment with brightness and contrast, *Mechanical Systems and Signal Processing*, **179**: 109363, doi: 10.1016/j.ymssp.2022.109363.
10. Liang L.Y., Chen S.M., Li P.R. (2020), The evaluation of vehicle interior impact noise inducing by speed bumps based on multi-features combination and support vector machine, *Applied Acoustics*, **163**: 107212, doi: 10.1016/j.apacoust.2020.107212.
11. Madvari R.F., Sharak M.N., Tehrani M.J., Abbasi M. (2022), Estimation of metal foam microstructure parameters for maximum sound absorption coefficient in specified frequency band using particle swarm optimisation, *Archives of Acoustics*, **47**(1): 33–42, doi: 10.24425/aoa.2022.140730.
12. Pourseiedrezaei M., Loghmani A., Keshmiri M. (2021), Development of a sound quality evaluation model based on an optimal analytic wavelet transform and an artificial neural network, *Archives of Acoustics*, **46**(1): 55–65, doi: 10.24425/aoa.2021.136560.
13. Shi W.K., Liu G.Z., Song H.S., Chen Z.Y., Zhang B. (2018), Vibration and noise characteristics of electric bus [in Chinese], *Jilin Daxue Xuebao (Gongxueban)*, **48**(2): 373–379, doi: 10.13229/j.cnki.jdxbgxb20170110.
14. Steinbach L., Altinsoy M.E. (2019), Prediction of annoyance evaluations of electric vehicle noise by using artificial neural networks, *Applied Acoustics*, **145**: 149–158, doi: 10.1016/j.apacoust.2018.09.024.
15. Wang C., Peng J.X., Zhang X.W. (2020), A classification method related to respiratory disorder events based on acoustical analysis of snoring, *Archives of Acoustics*, **45**(1): 141–151, doi: 10.24425/aoa.2020.132490.
16. Wang Y., Zhang S., Meng D.J., Zhang L.J. (2022), Nonlinear overall annoyance level modeling and interior sound quality prediction for pure electric vehicle with extreme gradient boosting algorithm, *Applied Acoustics*, **195**: 108857, doi: 10.1016/j.apacoust.2022.108857.
17. Wang Y.S. (2009), Sound quality estimation for non-stationary vehicle noises based on discrete wavelet transform, *Journal of Sound and Vibration*, **324**(3–5): 1124–1140, doi: 10.1016/j.jsv.2009.02.034.
18. Zhang E.L., Chen X.Y., Li S.Y., W Q.Q., Zhuo J.M. (2022a), A comprehensive evaluation model of electric

bus interior acoustic comfort and its application, *International Journal of Acoustics and Vibration*, **27**(4): 361–366, doi: 10.20855/ijav.2022.27.41887.

19. Zhang E.L., Chen Y., Chen X.Y., Zhang J.B., Xun P.W., Zhuo J.M. (2023a), High-precision modeling and prediction of acoustic comfort for electric bus based on BPNN and XGBoost, *International Journal of Acoustics and Vibration*, **28**(2): 158–164, doi: 10.20855/ijav.2023.28.21922.
20. Zhang E.L., Hou L., Shen C. (2016), Sound quality prediction of vehicle interior noise and mathematical modeling using a back propagation neural network (BPNN) based on particle swarm optimization (PSO), *Measurement Science and Technology*, **27**(1): 015801, doi: 10.1088/0957-0233/27/1/015801.
21. Zhang E.L., Zhang Q.M., Xiao J.J., Hou L., Guo T. (2018), Acoustic comfort evaluation modeling and improvement test of a forklift based on rank score comparison and multiple linear regression, *Applied Acoustics*, **135**: 29–36, doi: 10.1016/j.apacoust.2018.01.026.
22. Zhang E.L., Zhuo J.M., Hou L., Fu C.H., Guo T. (2021), Comprehensive annoyance modeling of forklift sound quality based on rank score comparison and multi-fuzzy analytic hierarchy process, *Applied Acoustics*, **173**: 107705, doi: 10.1016/j.apacoust.2020.107705.
23. Zhang X.C., Cheng J., Lu J.W., Yuan B., Jiang P., Sha W. (2022b), Sound quality evaluation of pure electric vehicle with subjective and objective unified evaluation method, *International Journal of Vehicle Design*, **88**(2–4): 283–303, doi: 10.1504/IJVD.2022.127024.
24. Zhang Y., Meng T., Wang K. (2020), Subjective evaluation model for interior sound quality and optimization of medium-frequency noise, *Automotive Engineering*, **42**(5): 651–657+664, doi: 10.19562/j.chinasae.qcgc.2020.05.013.
25. Zhang Y., Peng B.T., Yang E.C., Ren K.L., OU J. (2023b), Prediction and analysis of vehicle interior sound quality based on XGBoost algorithm [in Chinese], *Noise and Vibration Control*, **43**(3): 161–166+211, doi: 10.3969/j.issn.1006-1355.2023.03.025.